Electronic Supplementary Information

Laser Engineered Fabrication of Binder-Free NiCoFeCrZn-based High Entropy Oxide Electrode for Hydrogen Evolution Reaction in Alkaline Water

Electrode Fabrication Procedure:

An equimolar solution of metal nitrate precursors was prepared by dissolving 150 mg of $Ni(NO_3)_2 \cdot 6H_2O$, 150 mg of $Co(NO_3)_2 \cdot 6H_2O$, 208 mg of $Fe(NO_3)_2 \cdot 9H_2O$, 206 mg of $Cr(NO_3)_3 \cdot 9H_2O$, and 153 mg of $Zn(NO_3)2 \cdot 6H_2O$ in 10 mL of methanol. Aliquots of 66, 200, 400, and 660 µL of this solution were drop-cast onto a 4 cm^2 carbon cloth substrate to obtain electrodes with total metal loadings of 1, 3, 6, and 10 mg cm^{-2}, respectively. The resultant precursor-coated electrodes were subsequently annealed using a 30 W CO_2 laser operated at 10% power, 5% scanning speed, and 10% frequency. These optimized laser parameters facilitated the complete decomposition of metal salts while preserving the structural integrity of the carbon cloth substrate. The decomposition of metal salt at the surface of carbon cloth can be represented as follows:

$$M_x(NO_3)_y \xrightarrow{\Delta} M_xO_y + NO_2 \qquad (2)$$

Additionally, two more electrodes comprising of NiCo- and NiCoFe-oxide at equimolar metal concentrations were prepared to compare with the HEO-based electrode. This comparison is important to understand the cocktail effect of using five different metals in HEO. Prior to the electrochemical testing, all the electrodes were subjected to activation by cyclic voltammetry (CV). Precisely 2000 CV cycles were carried out at 100 mV s^{-1} between -0.9 to -1.8 V (v Hg/HgO) in 1.0 M KOH. Fig. S1 shows the CV activation curve of the optimized HEO/CC.

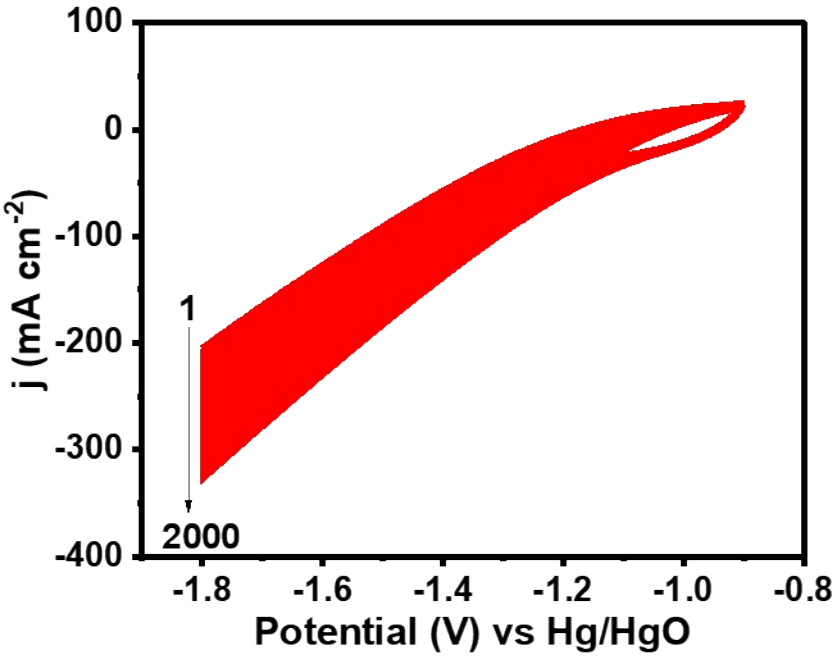

Fig. S1. CV curve of the HEO/CC electrode during activation in 1 M KOH.

Table S1. Entropy of mixing calculation using EDX atomic composition

i	**x_i**	**ln x_i**	**$-x_i$ ln x_i**
Ni	0.176	-1.73727	0.30576
Co	0.16	-1.83258	0.29321
Fe	0.223	-1.50058	0.33463
Zn	0.228	-1.47841	0.33708
Cr	0.212	-1.55117	0.32885
	S_{mix} =	**$-R\sum(x_i \ln x_i)$ =**	**1.59953R**

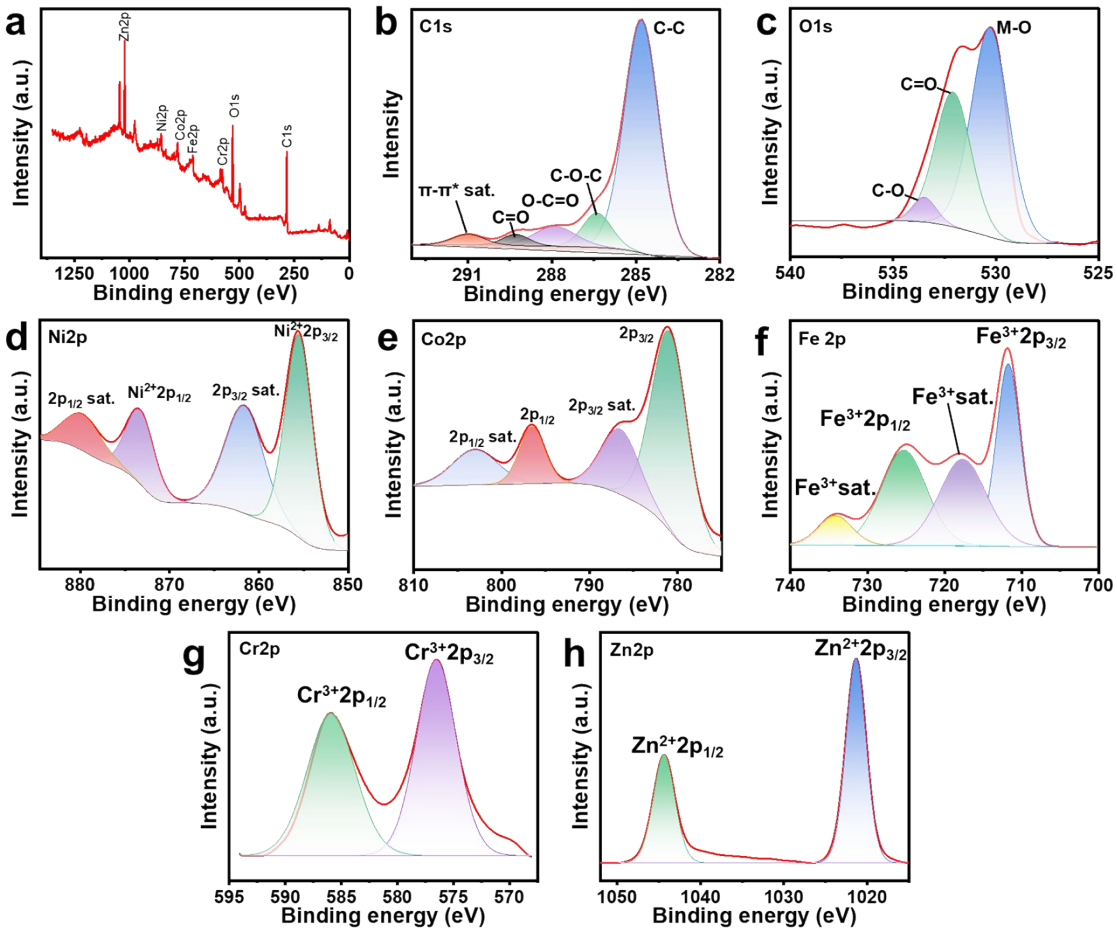

Fig. S2 XPS analysis of HEO/CC: (a) Survey spectra and respective high-resolution spectra (b) C1s, (c) O1s, (d) Ni2p, (e) Co2p, (f) Fe2p, (g) Cr2p and (h) Zn2p

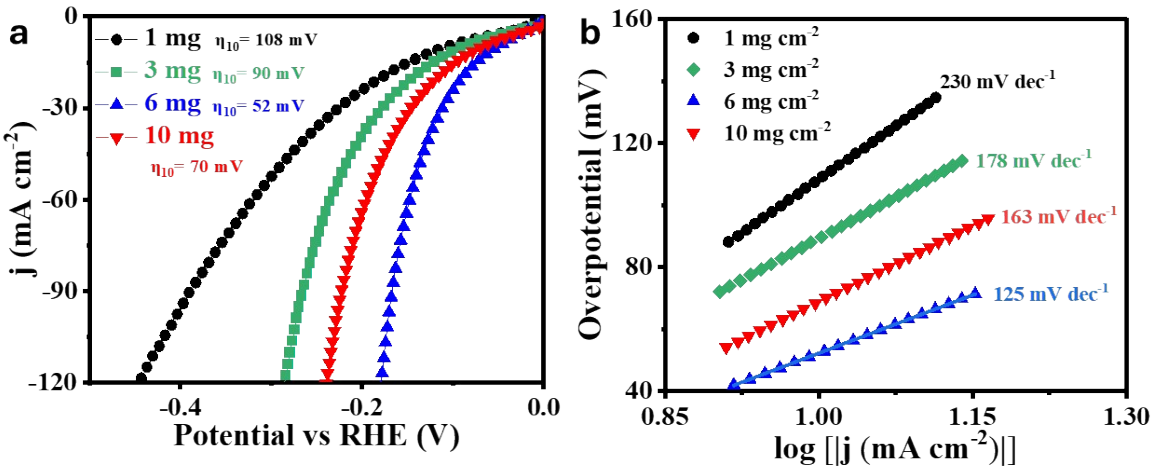

Fig. S3 (a) LSV polarization curves and (b) Tafel plots of HEO/CC at different catalyst loading.

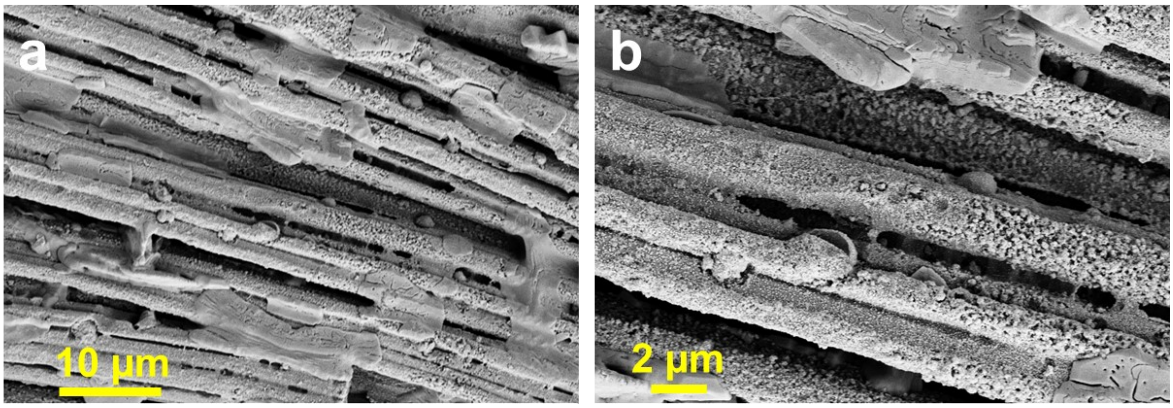

Fig. S4 (a) Low and (b) high magnification SEM images of HEO/CC at 10 mg cm^{-2} loading.

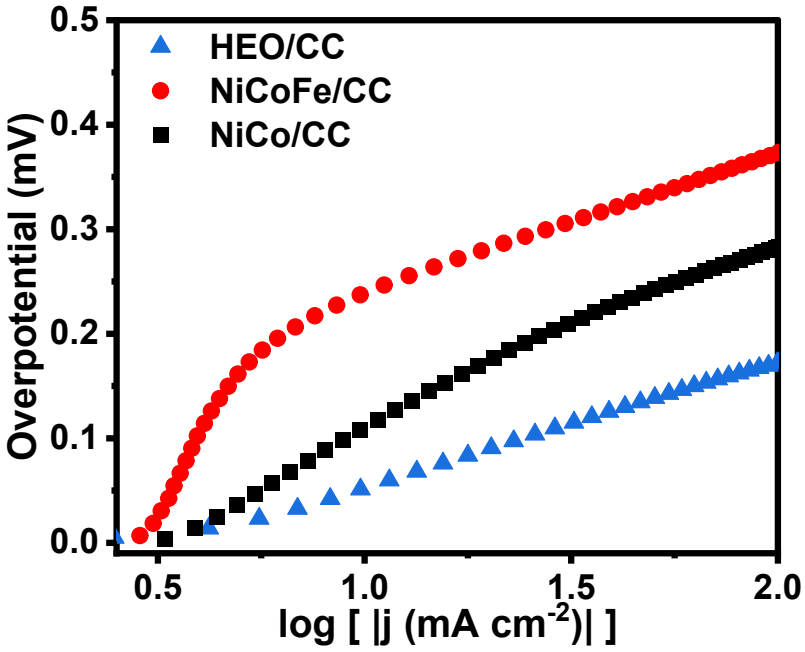

Fig. S5 Tafel plot of HEO/CC, NiCoFe/CC and NiCo/CC over the full current-density range.

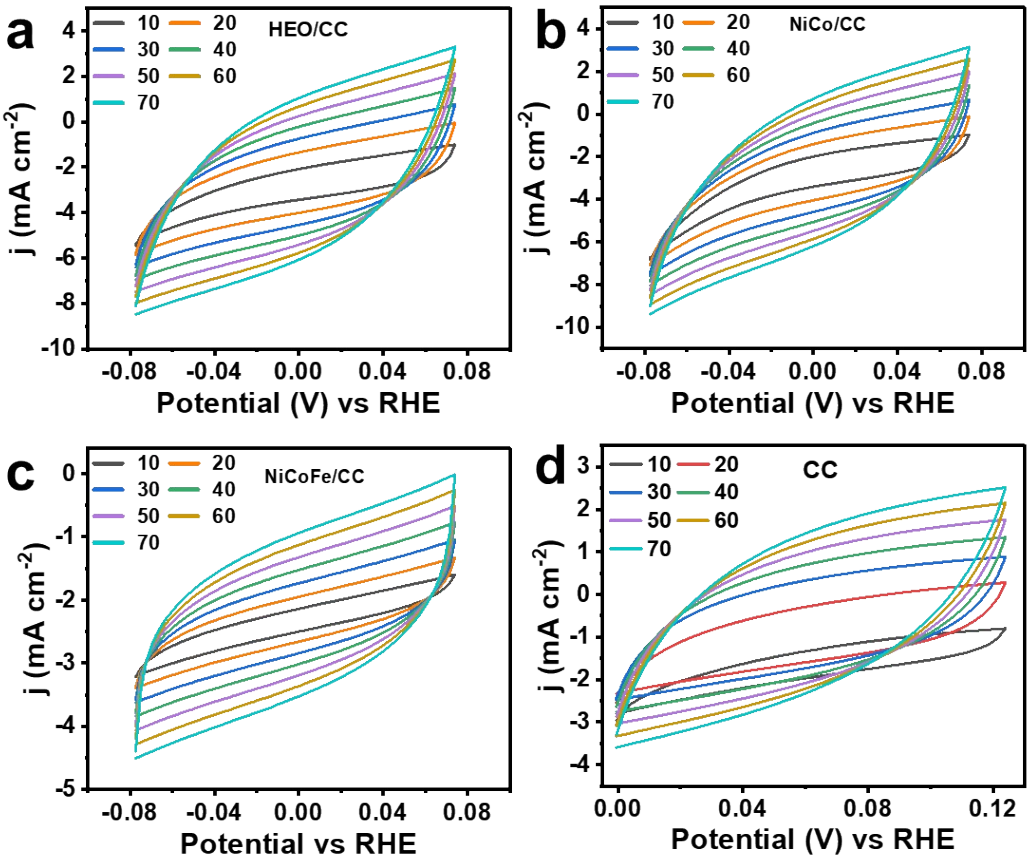

Fig. S6 CV plots of (a) HEO/CC, (b) NiCo/CC, (c) NiCoFe/CC and (d) CC, conducted at varying scan rates for C_{dl} measurements.

ECSA measurements

ECSA of the electrodes are determined by the following equation:

$$ECSA = E_{Geo}\frac{(C_{dl})_{eff}}{C_s}$$

Where,

E_{Geo} = Geometrical surface area

C_s = Specific capacitance = 10 to 60 µF cm^{-2}

$(C_{dl})_{eff}$ = Effective C_{dl} = Calculated C_{dl} of electrode – C_{dl} of the bare CC

The general value of Cs ranges from 10 – 60 µF cm^{-2}, an average value of 40 µF cm^{-2} is considered for calculation.

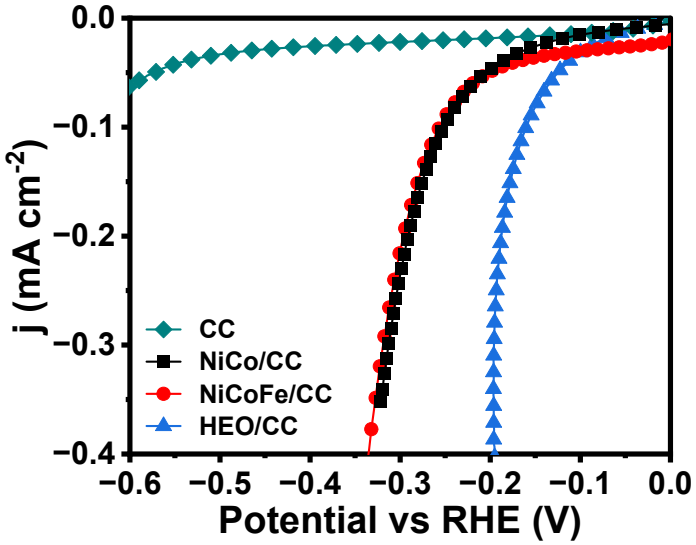

Fig.S7. Comparative ECSA normalized polarization plots of CC, NiCo/CC, NiCoFe/CC and HEO/CC.

Table S2: ECSA-normalized current density comparison across transition metal-based electrocatalysts at their corresponding evaluation potentials**.**

S.No.	Catalyst	j_{ECSA} (mA cm^{-2})	Potential (V) vs RHE	Ref.
1.	$(MoWVNbTa)_xC$	-0.10	-0.28	[1]
2.	FeCoNiMnRu	-0.14	-0.20	[2]
3.	Ni_3P MPs	-9.20×10^{-4}	-0.10	[3]
4.	Ni-Fe	-0.10	-0.26	[4]
5.	Pt-Ni3S2	-3.0	-0.20	[5]
6.	$Ru_{0.250}Ni$	-0.136	-0.30	[6]
7.	Ni_3N/Ni/CC	-0.10	-0.20	[7]
8.	$NiCo_2S_4/MoS_2$	-0.10	-0.29	[8]
9.	CoN/MoC/NMCNFs	-0.03	-0.37	[9]
10.	HEO/CC	-0.40	-0.20	This work

References

1. S. Niu, Z. Yang, F. Qi, Y. Han, Z. Shi, Q. Qiu, X. Han, Y. Wang, X. Du, S. Niu, Z. Yang, F. Qi, Y. Wang, Y. Han, Z. Shi, X. Du, Q. Qiu and X. Han, Adv. Funct. Mater., 2022, 32, 2203787.

2 G. Liu, C. Song, X. Li, Q. Jia, P. Wu, Z. Lou, Y. Ma, X. Cui, X. Zhou and L. Jiang, Chemical Engineering Journal, 2025, 509, 161070.

3 A. B. Laursen, R. B. Wexler, M. J. Whitaker, E. J. Izett, K. U. D. Calvinho, S. Hwang, R. Rucker, H. Wang, J. Li, E. Garfunkel, M. Greenblatt, A. M. Rappe and G. C. Dismukes, ACS Catal., 2018, 8, 4408–4419.

4 Z. Zhang, Y. Wu and D. Zhang, Int. J. Hydrogen Energy, 2022, 47, 1425–1434.

5 Z. Xing, D. Wang, T. Meng and X. Yang, ACS Appl. Mater. Interfaces, 2020, 12, 39163–39169.

6 W. Lian, F. Chen, J. Wu, H. Mo, Q. Zhu, X. Zhang, S. Song and F. Jia, Small, 2025, 21, 2406209.

7 L. Xiong, Y. Qiu, H. Dong, B. Gao, X. Zhang, P. K. Chu and X. Peng, Int. J. Hydrogen Energy, 2024, 59, 400–407.

8 S. Yu, R. Liu, R. Ma, Q. Zhou, Y. Dong, X. Lou, J. Pan and F. Xia, J. Alloys Compd., 2023, 932, 167678.

9 L. Wang, W. He, D. Yin, H. Zhang, D. Liu, Y. Yang, W. Yu and X. Dong, Renewable and Sustainable Energy Reviews, 2023, 181, 113354.